

A Model for the Drying Process During Film Formation in Waterborne Acrylic Coatings

Stefano Carrà¹*, Deborah Pinoci², Sergio Carrà²

¹Mapei S.p.A., Via Cafiero, 22, 20129 Milano (Italy)

²Dipartimento di Chimica Fisica Applicata, Politecnico di Milano, Via Mancinelli 7, 20131, Milano (Italy)

Summary: Establishing drying mechanisms during film formation in waterborne acrylic coatings is a technologically important problem, however complex, and still poorly understood. A model for the prediction of evaporation kinetics is proposed in this paper, where films are supposed to dry normally with respect to the film surface, and a drying front separates a top dry region from a bottom wet region. The model accounts for the competition between water evaporation and particle diffusion that determines the degree of vertical homogeneity, but also for the competition between water evaporation and particle deformation that ultimately establishes the rate-determining step in film formation processes. The model was validated by performing gravimetric water-loss experiments on latexes of acrylic polymers of various composition, various particle size and stabilizing systems, under different environmental temperatures and humidity, and various initial film thicknesses in order to evaluate the effect of the different factors that can in principle influence the film formation process.

Keywords: film formation; coatings; evaporation; acrylic latexes; mathematical modelling

Introduction

Establishing the mechanisms that govern drying during film formation is extremely important from a technological point of view for almost every coating application, but it is also a surprisingly complex and poorly understood problem, even if it has been frequently tackled in recent literature^[1]. Film formation is generally described as a sequence of three steps: a stable colloidal dispersion is applied to a substrate; as water evaporates, polymer particles become more and more concentrated until they reach maximum packing (step I); when the forces accompanying drying exceed the viscoelastic resistance of particles, these start to deform to yield a mechanically

weak void-free film, where the original particles are still distinguishable (step II); finally reptation across interparticle boundaries renders particles undifferentiated and generates the entanglements that provide mechanical strength to the film. Water evaporation during film formation is more complicated than what it looks intuitively. The most fundamental variable related to evaporation mechanisms is the rate of evaporation itself, around which disagreement and controversy still linger in literature: Vandezande and Rudin^[2] registered constant rates until particle concentrations around 93%, while Vanderhoff^[3] observed decreasing rates at much lower concentrations and final rates consistent with diffusion of water vapor through a continuous polymer layer. As pointed out by Winnik^[4], in order for a continuous layer to be able to restrain evaporation, polymer particles must be easily deformable. A brutal simplification in the description of drying phenomena would be to consider it homogeneous, meaning that water concentration remains uniform during the whole process. Dilute dispersions usually start drying homogeneously, but at a certain concentration dishomogeneities usually appear, as a consequence of several possible factors, among which the most significant are probably the presence of diffusional limitations that create particle concentration profiles from the beginning of the process, but also the possibility that, once maximum packing has been reached, the level of water might recede in the film, leaving a dry film layer on top, resting on a wet layer^[5]. Much interest has also been drawn by the problem of drying fronts that can move normally to the film surface, but also propagate laterally^[6]. In these conditions, and depending on the deformability of particles, the top of the film might reach a volume fraction of unity (no voids) before the rest of the film, sometimes before the rest of the film has even reached maximum packing. A useful criterion to understand the deformation behavior was proposed by Routh et al.^[7], by comparing the evaporation time, nominally H/\dot{E} , where H is the initial film thickness and \dot{E} the rate of evaporation, with the time scale for deformation $\tau = \eta_0 R_0 / \gamma_{pw}$, where η_0 is the viscosity of a melt of the latex polymer, R_0 is the particle radius and γ_{pw} the water-air interfacial tension. Temperature, or rather the difference $T - T_g$, where T_g is the gel transition temperature of the polymer, influences greatly η_0 , and hence the overall deformation behavior.

There is a great applicative scope for the development of a model capable of describing the drying of water throughout the film formation process, at different environmental temperature and

humidity, different coating thicknesses, and various latex properties (T_g , particle size distribution, stabilization type, eventually particle morphology), like the one proposed in this paper. Model results have been validated by the comparison with a series of experimental results.

Experimental

In this work the evaporation kinetics in film formation processes was investigated using several different acrylic latexes. These latexes were both laboratory prototypes and industrial products, with different monomeric composition and solid content, and various stabilizer types and amounts. The T_g of the different polymers was measured by Differential Scanning Calorimetry, on a Mettler Toledo TC 15 Thermoanalyser. Latex solid content was determined by gravimetry. Latex particle size distribution was estimated via light scattering using a LS-230 Coulter Particle Analyzer. Latex viscosity was determined using a Haake Viscotester VT5. Evaporation kinetics during film formation was determined adopting a gravimetric technique, registering on a scale connected on-line to a computer the loss of weight of a latex sample while this is drying on a glass plate. Borders were built on the glass plate by applying one or more layers of adhesive tape, in order to control the film thickness. Data were registered every 10 s. The control of the velocity of the air flow onto the sample was guaranteed by assembling a small wind tunnel where a series of small tubes convey air from a fan. It is important to check, using an anemometer, that all experiments are performed at a constant air velocity ($\cong 4$ m/s in the experiments described in this paper). The apparatus was located inside a climatic chamber where it was possible to vary environmental temperature and humidity, within certain limits ($10 \div 40$ °C, $30 \div 70\%$ r.h.).

Results

Raw experimental data are given in terms of sample weight vs. time. Rates of evaporation can be calculated by numerical derivation. The solid content ϕ of the sample at every instant during the experiment can be calculated through a water mass balance, using the final solid content as a reference point. Experimental data are better compared in terms of the adimensional variable τ , defined as the time required to evaporate a certain amount of water from the latex divided by the

time required to evaporate the same amount of water as pure water. Figure 1 shows a series of experimental τ vs. ϕ curves as obtained by drying an acrylic latex with a T_g of 20°C, with different environmental temperature, above and below the T_g . It is possible to observe that environmental temperature does not have any influence on the drying process until very high values of ϕ are reached. In any case the beginning of decreasing rate period is anticipated when drying is performed at high temperature, probably due to the stronger influence of diffusional limitations at higher rates of water evaporation. Evaporation hindrance increases when the temperature is set above the polymer T_g , due to the increased deformability of particles.

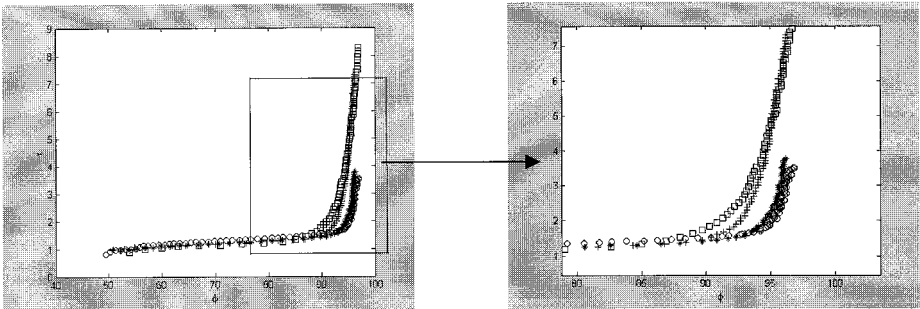


Figure 1. Experimental τ vs. ϕ curves (complete curved on the l.h.s, zoomed in on the r.h.s.) as obtained by drying an acrylic latex with a T_g of 20°C, with different environmental temperature (o: 10 °C, *: 20 °C, +: 30 °C, □: 40 °C).

Figure 2 shows experimental curves as obtained by drying an acrylic latex with a T_g of -39°C, by varying initial thickness. Results show that evaporation hindrance increases with initial thickness as an effect of diffusional limitations, and that the film with initial thickness equal to 1.5 requires a really long time to dry.

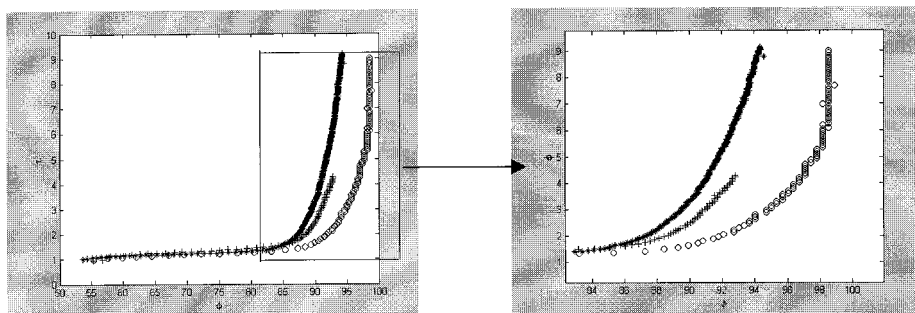


Figure 2. Experimental τ vs. ϕ curves (complete curved on the l.h.s, zoomed in on the r.h.s.) as obtained by drying an acrylic latex with a T_g of -39°C , with different initial thickness (\circ : 0.5 mm, $+$: 1 mm, $*$: 1.5 mm).

Figure 3 shows experimental curves as obtained by drying two different acrylic latexes with the same monomeric composition and a T_g of -39°C but different stabilizing system one prevalently anionic and the other prevalently non-ionic, where it is possible to notice that the former shows a lower evaporation hindrance, probably due to the fact that the electrostatic stabilization potential produced by the anionic emulsifier is more efficient in hindering and delaying particle deformation.

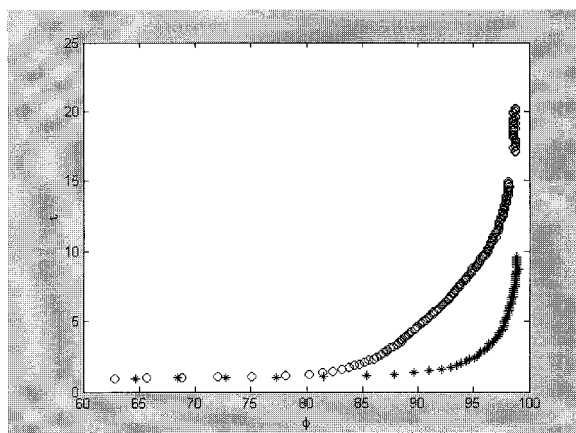


Figure 3. Experimental τ vs. ϕ curves as obtained by drying two different acrylic latexes with the same monomeric composition and a T_g of -39°C but different stabilizing system ($*$: prevalently anionic; $^\circ$: prevalently non-ionic).

Figure 4 shows experimental curves as obtained by drying, at 20 °C, 50% of relative humidity and 1 mm of initial thickness, three different acrylic latexes. The latex at lower T_g displays the maximum evaporation hindrance, while the other two, that have similar T_g , almost tend to overlap, even if initial concentrations are very different.

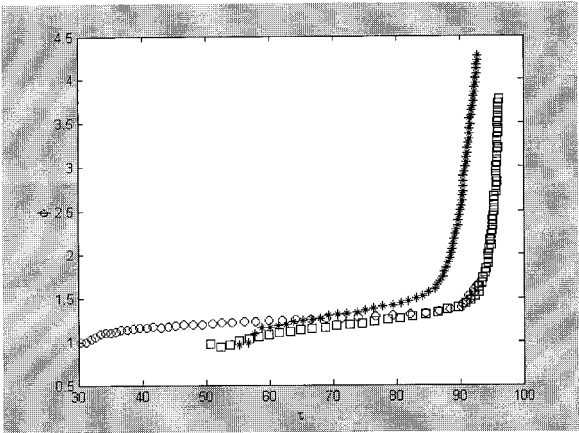


Figure 4. Experimental τ vs . ϕ curves as obtained by drying three different acrylic latexes (o: $T_g = 19.3$; □: $T_g = 20.0$; *: $T_g = -39.0$).

Mathematical Model

Effect of Diffusion Limitations

By developing the equations derived by Russel^[8] to describe the diffusion we derived the following differential equation to describe vertical dishomogeneities during film formation:

$$\frac{\partial \phi}{\partial t} = D \frac{\partial^2 \phi}{\partial z^2} \tag{1}$$

relying on the hypothesis the sedimentation is neglectable.

Partial differential equation (1) can be solved using the method of the separation of variables, that, imposing the initial condition:

$$\phi(z,0)=\phi_0 \tag{2}$$

leads to:

$$\phi(z,t)=\phi_0 e^{az} e^{\alpha^2 D t} \tag{3}$$

Where α is the parameter introduced for the solution of the differential equation.

It is necessary to impose the condition that ϕ cannot surpass maximum packing fraction ϕ_{\max} , i.e. 0.73 for monodisperse latexes, therefore:

$$\begin{aligned}\phi(z, t) &= \phi_0 e^{\alpha z} e^{\alpha^2 D t} \quad \text{for } z < z^* \\ \phi(z, t) &= \phi_{\max} \quad \text{for } z \geq z^*\end{aligned}\tag{4}$$

where z^* is the coordinate at which the calculated ϕ is equal to ϕ_{\max} .

The position of the film-air interface is defined by the variable h , that can be easily calculated by a water mass-balance:

$$-\frac{dh}{dt} = V_{ev}(t)\tag{5a}$$

with the initial condition:

$$h = h_0 \quad \text{at } t = 0\tag{5b}$$

where V_{ev} is the rate of water evaporation, in m/s.

The mass balance for solid particles would be satisfied by equating the average value of ϕ , as defined in equation (4):

$$\bar{\phi} = \frac{1}{h} \left\{ \frac{\phi_0 e^{\alpha^2 D t}}{\alpha} \left[e^{\alpha z^*} - 1 + 0.75(h - z^*) \right] \right\}\tag{6}$$

with

$$\bar{\phi} = \frac{h^0 \phi^0}{h(t)}\tag{7}$$

By imposing this condition, we can calculate α . An example of calculation from the model developed above is given in Figure 5, where $\phi(z)$ profiles are shown at increasing values of t , for a set of parameters, $D = 1 \times 10^{-16}$ [m²/s], $h = 1 \times 10^{-3}$ [m], $U = 5 \times 10^{-8}$ [m/s], that corresponds to a value of the adimensional variable $HU/D = 2500 \gg 1$, that should lead to strong dishomogeneities in the film. Profiles are in fact very steep, and maximum packing at the film-air interface is reached when $\bar{\phi}$ is still in the order of 0.5.

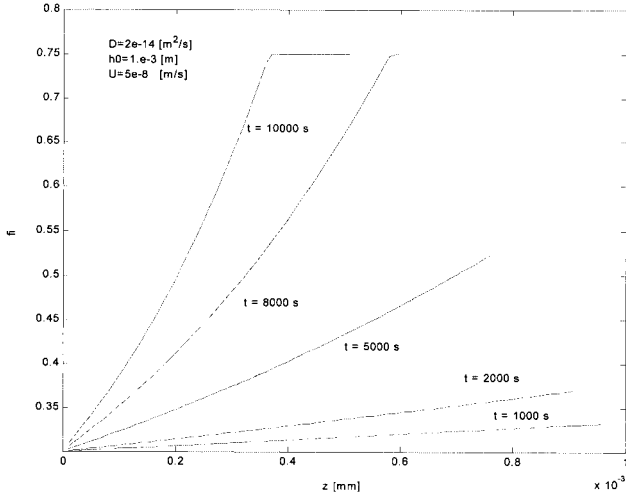


Figure 5. $\phi(z)$ profiles at increasing values of t , for a set of parameters, $D = 1 \times 10^{-10}$ [m²/s]; $h_0 = 1 \times 10^{-3}$ [m]; $U = 5 \times 10^{-8}$ [m/s].

Effect of particle packing and deformation on evaporation kinetics

Evaporation is supposed to take place at a constant rate, approximatively equal to the rate evaporation of pure water, as long as the film-air interface is below maximum packing. Expressed in moles of water per unit area and time:

$$\tilde{N} = k_g [P^0(T)\gamma - P_A] \quad (8)$$

where k_g is the mass transfer coefficient [moles/(s cm² atm)], $P^0(T)$ is the water vapor pressure at temperature T , P_A is the water partial pressure in air, γ is an activity coefficient to take into account possible effects of water soluble polymer, eventually present, onto vapor pressure.

At maximum packing, particles undergo deformation driven by capillary pressure, opposed by their elastic resistance. Described as a purely elastic phenomenon, deformation is supposed to be instantaneous. This is not the case if, more correctly, their viscoelastic character is taken into account.

At a certain point during the film formation process, as dictated by a water mass balance, the water-air interface starts receding inside the film, leaving a layer of dried deformed particles above. Even when in a dry state particles keep on deforming by dry sintering, driven by the

polymer-air interfacial tension, and opposed by the viscous characteristic of the polymer. The situation at an instant t is represented in Figure 6:

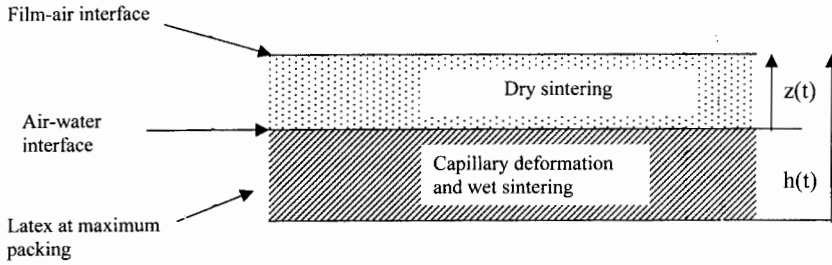


Figure 6. Schematic of inhomogeneous drying

The state of packing and deformation at a height z in the film can be defined by a variable $\varepsilon(z, \tau)$, that is essentially the degree of void, where τ is the time, relative to the instant at which the layer of particle at level z has reached maximum packing. Eckersley and Rudin^[9] proposed a model where the contact radius of particles during stage II is the sum of contribution from the capillary and interfacial force.

$$a = a_{\text{capillary}} + a_{\text{interfacial}} = (2.8 R^2 \sigma / G^*)^{1/3} + (3 \gamma R t / 2 \pi \eta^*) \quad (9)$$

Contact radius and degree of void are related by a geometric relationship:

$$\varepsilon = 1 - \frac{4 + 2z^2 - 0.083z(3\xi^2 + 0.25z^2)}{1.333 + 4(1 - 0.5z)} \quad (10)$$

where $(a/R) = \xi$ and $z = 2(1 - \sqrt{1 - \xi^2})$.

Therefore the instantaneous degree of void can be expressed as a sum, on an initial contribution that is complementary to the situation of maximum packing that identifies the condition at which deformation begins, of an instantaneous contribution due to capillary deformation, ε_c , and a time dependent contribution due to dry sintering:

$$\varepsilon(\zeta, \tau) = \varepsilon_0 + \varepsilon_c + \varepsilon(\tau) \quad (11)$$

Where $\varepsilon_0 = 1 - \phi_{\max}$. The dry film layer is therefore characterized by a profile of $\varepsilon(z)$, and forms an obstacle to the evaporation of water from the air-water interface below, that can be expressed in terms of a pressure drop ΔP . The rate of evaporation of water is therefore:

$$N = k_g (P^0 \gamma - P_A - \Delta P) \quad (12)$$

The pressure drop in the dry layer can be described as it was in a porous bed:

$$\frac{dP}{dz} = - \frac{1}{K \Psi[\varepsilon(t)]} u^{(g)} \quad (13)$$

where $u^{(g)}$ is the gas velocity $u^{(g)} = N / \tilde{\rho} \varepsilon(t)$. Parameter K is defined as d_p^2 / μ , d_p being the particle diameter and μ the latex viscosity. Several different functions have been proposed in the literature for function Ψ . We applied the classic Ergun's equation, according to which:

$$\Psi[\varepsilon(t)] = \frac{\varepsilon^3}{180(1 - \varepsilon)} \quad (14)$$

Defining as $Z(t)$, the thickness of the dry state, it is:

$$dZ = u^{(l)} dt \quad (15)$$

where $u^{(l)}$ is the liquid velocity. Continuity equation states that:

$$u^{(l)} \varepsilon^0 \tilde{\rho}^{(l)} \Omega = u^{(g)} \varepsilon(t) \tilde{\rho}^{(g)} \Omega \quad (16)$$

By integrating (11), and using (13) and (14), we derive:

$$\Delta P = - \int_0^Z \frac{u^{(g)}}{K \Psi[\varepsilon(t)]} dz = \frac{\tilde{\rho}^{(g)}}{\tilde{\rho}^{(l)} \varepsilon^0} \int_0^t \frac{u^{(g)^2} \varepsilon(t)}{K \Psi[\varepsilon(t)]} dt \quad (17)$$

Evaporation kinetics in the presence of a dry upper state is then described by the following equations:

$$u^{(g)}(g) = \frac{k_g}{\tilde{\rho}^{(g)} \varepsilon(g)} \left[(P^0 \gamma - P_A) - \frac{\tilde{\rho}^{(g)}}{K \tilde{\rho}^{(l)} \varepsilon^0} \int_0^g \frac{u^{(g)^2} \varepsilon(\tau)}{\Psi[\varepsilon(\tau)]} d\tau \right] \quad (18)$$

$$\frac{dZ}{dt} = \frac{k_g}{\tilde{\rho}^{(l)} \varepsilon^0} \left[(P^0 \gamma - P_A) - \frac{\tilde{\rho}^{(g)}}{K \tilde{\rho}^{(l)} \varepsilon^0} \int_0^g \frac{u^{(g)^2} (g) \varepsilon(g)}{\Psi[\varepsilon(g)]} dg \right] \quad (19)$$

Simulations and comparisons with experimental data

Two examples of comparisons between simulations and experimental data are given in the two Figure 7 and 8. In Figure 7 rate vs. time curves are shown for a acrylic latex latexes with a T_g of -39°C and a 58% solid content at two different initial film thickness. In Figure 8 rate vs. time curves are shown for a latex of a polyvinyl acetate butyl acrylate copolymer with a T_g of 20°C and a 55% solid content at three different initial film thickness.

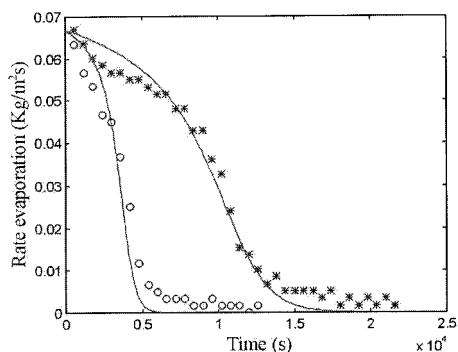


Figure 7. Rate vs. time curves for a acrylic latex latexes with a T_g of -39°C and a 58% solid content at two different initial film thickness (o: 0.5 mm, *: 1mm).

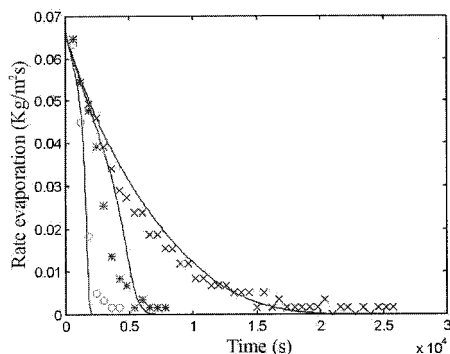


Figure 8. Rate vs. time curves are shown for a latex of a polyvinyl acetate butyl acrylate copolymer with a T_g of 20°C and a 55% solid content at three different initial film thickness (o: 0.2 mm; *: 0.5 mm; x: 1 mm)

The agreement between model predictions and experimental data is striking, but it has been

obtained optimising somehow the values of G^* and η^* , in the range of values obtained by DMA, since the shortcomings of our model are somehow similar to those of Eckerling's and Rudin's^[9], and the time scales of the deformation and flow processes are not exactly known. However our model takes explicitly into account the competition of particle deformation and water evaporation, and therefore it is able to discriminate if film forms under the effect of dry rather than dry mechanisms, and if a dry G^* should be used, rather than wet (wet values of G^* are lower, due to plasticization).

Conclusions

Establishing drying kinetics during film formation is a problem that is important as it is difficult. Results from a series of gravimetric experiments have been shown, demonstrating the effect on drying kinetics of environmental conditions and latex properties. A model to predict the rate of evaporation of water in a system where water evaporated normally to the film surface was proposed in this paper, showing excellent agreement with experimental results, but the estimation of some model parameters is critical, and should be further addressed in order to obtain a fully predictive model.

References

- [1] Y. Holl, J. L. Keddie, P. J. McDonald, W. A. Winnik, in "Film Formation of Coatings"; T. Provder, M. W. Urban, Eds., ACS Symposium Series; American Chemical Society: Washington DC, Vol. 790, 2001, p. 2
- [2] G. A. Vandezande, A. Rudin, *J. Coat. Tech.* **1996**, 68, 63
- [3] J. W. Vanderhoff, H.L. Tarkowski, M.C. Jenkins, E.B. Bradford, *J. Macrom. Chem.*, **1966**, I, 361
- [4] M. A. Winnik, *Emulsion Polymerization and Emulsion Polymers*, Editors: P. A. Lovell, M. S. El-Aasser, John Wiley and Sons, 467 (1997)
- [5] A.F. Routh, W.B. Russel, *AIChE J.*, **1998**, 44, 2088
- [6] M. A. Winnik, J. Feng, *J. Coat. Tech.*, **1996**, 68, 39
- [7] A.F. Routh, W.B. Russel, J. Tang, M. S. El-Aasser, , *J. Coat. Tech.*, **2001**, 73, 41
- [8] W. B. Russel, D. A. Saville, W. R. Schowalter, "Colloidal Dispersions", Cambridge University Press, 1992
- [9] S.T. Eckersley, A. Rudin, in "Film Formation in Waterborne Coatings", T. Provder, M. A. Winnik, M. W. Urban, Eds., ACS Symposium Series; American Chemical Society: Washington DC, Vol. 648, 1996, p. 2